JOURNAL OF EXPERIMENTAL AND THEORETICAL PHYSICS, 2024, Vol. 166, No. 6 (12), pp. 867–878

STATISTICAL, NONLINEAR, AND SOFT MATTER PHYSICS

FRACTAL STRUCTURE OF A SPRUCE BRANCH

© 2024 S. V. Grigoriev[a,b]*, O. D. Shnyrkov[a,b], K. A. Pshenichnyi[a], E. G. Yashina[a,b]

[a] Petersburg Institute of Nuclear Physics named after B. P. Konstantinov of the National Research Center "Kurchatov Institute", Leningrad Region, Gatchina, 188300 Russia

[b] Saint Petersburg State University, Saint Petersburg, 198504 Russia

* e-mail: grigoryev_sv@pnpi.nrcki.ru

Received July 17, 2024

Revised August 26, 2024

Accepted August 26, 2024

Abstract. The fractal properties of the spruce branch structure were studied using numerical Fourier analysis. Images of spruce branches from a mature 26-year-old spruce tree, about 13 m in length, were studied at various tree heights. For different branches photographed in various projections, a power-law dependence of spectral intensity $I(q) = Aq^{-N}$ is observed, where $N = 2$ in the momentum range q from 0.07 to 2 cm^{-1}. Such power law defines the characteristic structure of a spruce branch, described by a logarithmic fractal in twodimensional space in the size range from 5 to 100 cm. The discovered structure represents the distribution of needles on the spruce branch and is related to its photosynthesis function. The transport functions of the branch are provided by the branching structure of twigs, which is described by a classical fractal with dimension $1 < D_f < 2$ in the same momentum range from 0.07 to 2 cm^{-1}.

DOI: 10.31857/S004445102412e125

1. INTRODUCTION

Many objects found in nature are so highly fragmented and fractured that it is impossible to accurately describe them within the framework of classical geometry. To precisely describe such objects, in the second half of the twentieth century, Benoit Mandelbrot introduced the term "fractal" and constructed a new, unusual "fractal geometry of nature" [1]. His proposed concept very quickly gained widespread use and began to be applied in various fields of science and technology (from radio electronics to medicine) [2–11]. Fractal objects, in addition to fragmentation, are characterized by another property: self-similarity. The main characteristic of fractal objects is the fractal dimension, which is used to classify these objects when describing nontrivial properties of their structure. The relevance of tasks both in studying fractals through experimental methods and in developing fractal theory is due to the prevalence of objects with fractal properties, as well as the wide field of application of the fractal concept. There are many examples where the structure of biological systems or processes within them can be described using fractal dimension. Fractal patterns within living organisms are used for disease diagnosis and prediction of potentially dangerous conditions [11–14].

One of the most illustrative, yet controversial examples of fractal geometry in nature is a tree [15–21]. The modern basis for describing the structure of trees is the metabolic scaling theory, which was proposed in the works of West and co-authors [22, 23]. The theory, as applied to plants, is based on the premise that water transport is a concomitant limiting factor for photosynthesis. Since water transport is largely a physical process, partially dependent on the structure of the transport network, its scaling can be predicted using relatively simple allometric models, leading to scaling predictions for all dependent metabolic processes. West's model [22, 23] is quite simple in its construction. The branching structure of a plant is divided into external and internal components. The external structure follows symmetrical and selfsimilar branching, which allows for easy scaling of the structure. The external structure also corresponds to biomechanical principles of area preservation and safety from gravitational buckling. The internal branching structure represents a network of xylem

channels within the branches. The number and sizes of xylem channels are connected by simple rules to the external network of branches. Thus, it is assumed that the fractal geometry of trees is a direct reflection of both internal and plastic, morphological and physiological characteristics that govern the growth and survival of trees. Therefore, fractal geometry provides a unique way to quantitatively describe the structural complexity of tree crowns — the assemblage of branches and foliage on them. In the model, one can assume that the vascular networks of trees represent "space-filling" fractal networks of their branches. That is, tree branches are fractallike or self-similar at different scales, with self-similarity in branching implying that any branching point looks the same regardless of whether we observe the first or last branching point of the tree.

An experimentally verified description of tree structure using the fractal concept has remained unattainable until recently, and only lately methods have emerged that clearly demonstrate the fractal characteristics of trees [24–27]. In the vast majority of works on the fractal properties of trees, researchers sought to propose a model (a theoretical model) of a tree-like object. Then an attempt was made to determine the fractal dimension of the resulting artificial construct – a 'golem' intended to qualitatively simulate a real tree. Naturally, such attempts lead to results that can only approximately be associated with trees.

In our opinion, conducting experiments with real trees is absolutely necessary not only to verify the proposed models but also, not least, for experimental guidance regarding the subject of research itself: which part of the tree should be considered fractal – the configuration of leaf placement or the branching structure without considering foliage? The experiment is also capable of directly indicating the presence of fractal patterns, including the spatial limits within which it is observed. Indeed, the self-similarity of branches is not preserved at all levels of branching hierarchy in deciduous trees [25, 26], and old branches and young branches should be considered separately [27]. The criterion for division into young and old branches can be the presence/absence of foliage on the branches. That is, young branches are direct participants in photosynthesis, while old branches carry the functions of the transport system in the whole tree organism. This noticeably changes their structural characteristics, which is reflected in the experiment [26, 27]. In other words, experimental methods for determining the fractal dimension of an object are key to solving the problem of describing fractal properties in the structure of botanical trees.

There are several methods for experimental assessment of the fractal dimension of trees, which, however, depend on the model describing certain aspects of the tree – leaf cover, branching system, etc. [15, 19]. Allometric models provide a quantitative description of the spatial structure of trees and associated metabolic processes through scaling relationships of significant tree parameters. For example, in works [22, 23] it was shown that the metabolic rate B scales with tree mass M to the power of 3/4 (i.e., $B \sim M^{3/4}$). This scaling prediction can be broken down into two separate components that individually relate mass and water consumption to the easily measurable trunk diameter D. This concept relies on the image of a tree as a symmetrical self-similar object. However, the fractal dimension of such an object remains undetermined, apparently due to the complexity and multi-component nature of the entire problem. Developing this approach, work [28] proposed evaluating the "path ratio" metric, which quantitatively determines the extent to which the branch network of a "real" tree differs from an ideal self-similar network. The path ratio metric P_f is defined as the ratio of the average path from the butt to the edge of the last branch to the maximum such path. The value P_f turns out to be equal to 1, $P_f = 1$, for a symmetrical self-similar tree. Such a construction in nature is characteristic of some oak varieties or for spherical willow. The tree becomes asymmetrical if $P_f = 2/3$ or $P_f = 1/2$, at which point a trunk begins to form and the tree resembles a birch in shape. In the case of $P_f = 1/3B$, the trunk dominates the tree shape and can be characterized as a spruce in form. It turned out that using such a metric, whose value ranges from 0 to 1, one can characterize the shape of a tree. However, this does not determine which part of the tree is fractal, and, of course, does not determine the fractal dimension of the tree. Moreover, such a network is constructed from linear (path) rather than volumetric elements, and therefore the "tree" constructed in this way turns out to be already a generalized tree, far from reality.

There is a method for estimating the fractal dimension of trees using the "two surfaces" method [29, 30], which assumes that the fractal

dimension of a tree crown can be obtained from the relationship between the total leaf area of the tree and the surface area covering the crown. This estimation method can be extended, and the crown volume can be considered as the volume jointly occupied by both leaves and branches [31]. In this estimation, the fractal dimension takes values from 2 to 3, where a dimension equal to 2 means that the foliage is distributed along the periphery of the crown, and the crown surface represents a classical flat Euclidean surface. As the fractal dimension increases (i.e., when the fractal dimension is greater than 2), the crown surface becomes more fractal until the fractal dimension becomes equal to 3, when the leaf surface is uniformly distributed in a given crown volume [29, 31] (analogous to the Peano curve in three-dimensional space). Typical values of fractal dimension in such measurement constitute $D = 2.2–2.3$, which indicates a tendency for the foliage cover to be located on the periphery of the tree crown [19]. It is obvious that this method rather speaks about the fractal dimension of the leaf mass on the tree and, possibly, indirectly about young branches covered with leaves, but does not provide information about the structure of the entire tree and its branching pattern.

The most well-known method of determining the structural complexity of trees based on fractal analysis is the volume coverage metric (in 3D space) occupied by tree branches, depending on the size of the ε covering element. Experimentally, such measurement can be conducted using laser scanning of the three-dimensional tree structure [24, 25], and the obtained fractal dimension in this case can vary from 1 to 3. Similar coverage technique is also applicable for two-dimensional tree images [32]. However, in the case of evergreen broadleaf trees, branches and trunk are hidden by foliage, and one has to reconstruct the fractal dimension of the object based on the fractal properties of the tree image boundary, i.e., based on the fractal properties of its surface. The disadvantages of this approach include the fact that it provides an estimate of the fractal dimension of the entire object based only on measurements of peripheral areas covered with foliage. This approach is not applicable for deciduous trees, which have a more complex structure with different fractal dimensions at different scales, as established in [25].

Nevertheless, fractal analysis is applicable to images of trees without foliage (in winter), when one can focus on tree branching patterns rather than its leaf cover [26, 27]). The fractal structure of an object in two-dimensional space can be studied from its image using numerical Fourier analysis, thus modeling an experiment of small-angle light scattering on a twodimensional object [33–38]. This method consists in finding and studying the spatial characteristics of the Fourier image of the studied image [39]. The use of numerical Fourier analysis has shown [26] that lateral projections of deciduous trees at scales corresponding to mature branches are logarithmic fractals, which are characterized by the law of surface area equality at all levels of mature branch ramifications. Moreover, it turned out that young branches differ in their fractal structure from mature ones [27]. It should be especially emphasized that the reason for the observed scaling laws of Fourier images of tree silhouettes (two-dimensional projections) is the quasi-two-dimensional structure of the wood layer, which provides water supply and nutrients to the tree.

Coniferous tree species with monopodial branching, which leads to the formation of a powerful trunk and numerous branches on it, have been much less frequently studied using fractal analysis. In this case, a single branch should be considered as an object of fractal geometry. Of particular interest is the question of how branches (identical in their structure and morphology) are distributed along the trunk. For a solitary spruce tree, it is assumed that its branches are distributed uniformly along the trunk in height and uniformly in azimuth around the trunk axis. In works [18, 40, 41], a method was proposed for determining the fractal dimension of a spruce branch. The branch was considered as an object constructed from linear segments, and to determine the fractal dimension, the total length of branches at each branching level was evaluated. Formulas in the form of convergent power series were proposed for calculating the total length of spruce branches depending on the branching level, and sequential calculations of the total branch length were performed at different scales. The fractal dimension was determined as the tangent of the slope angle of the line approximating the relationship between the scale unit of measurement and the total length of branches in a double logarithmic scale. Calculations were performed taking into account the dynamics

of branching level was evaluated. Formulas in the form of convergent power series were proposed for calculating the total length of spruce branches depending on the branching level, and sequential calculations of the total branch length were performed at different scales. The fractal dimension was determined as the tangent of the slope angle of the line approximating the relationship between the scale unit of measurement and the total length of branches in a double logarithmic scale. Calculations were performed taking into account the dynamics of branch growth and shoot dieback, as well as various lighting levels. It was noted [40] that the analytical expression for estimating the fractal dimension of a branch considering its needles becomes difficult. On the one hand, needles do not increase the fractal dimension of the branch at all, and on the other hand, they significantly increase the surface area. The role of needles in the overall fractal structure of the branch remained unclear. In any case, the results of fractal analysis obtained in works [18, 40, 41] are based on a one-dimensional branch model and do not take into account the fact that the branch has a finite surface area and finite volumebranch growth and shoot dieback, as well as various lighting levels. It was noted [40] that the analytical expression for estimating the fractal dimension of a branch considering its needles becomes difficult. On the one hand, needles do not increase the fractal dimension of the branch at all, and on the other hand, they significantly increase the surface area. The role of needles in the overall fractal structure of the branch remained unclear. In any case, the results of fractal analysis obtained in works [18, 40, 41] are based on a one-dimensional branch model and do not take into account the fact that the branch has a finite surface area and finite volume.

In our work, we provide an experimental assessment of the fractal dimension of spruce branches based on their images. To measure the fractal dimension, we use the method of numerical Fourier analysis of images. This experimental approach takes into account the surface area of the spruce branch together with its needles when measuring. It has been established that spruce paws, framed by needles, are formed according to the law of logarithmic fractal in two-dimensional space, i.e., they follow the rule of conservation of the total branch area before and after branching.

It should be noted that until now, no connection has been established between the results of metabolic scaling theory and experimentally obtained values of the fractal dimension of trees. At the same time, our approach will apparently provide results that will establish such a connection in the near future.

The work is organized as follows. Section 2 presents a study using numerical Fourier analysis of images of branches from a 26-year-old spruce at different trunk heights. Section 3 provides results of the analysis of the fractal dimension of branches framed by needles. Section 4 compares the obtained experimental results with the results of the theoretical model [18, 40, 41]. Section 5 presents the conclusions of the work.

2. RESEARCH METHODOLOGY

A spruce paw represents a quasi-two-dimensional object, based on a hierarchical monopodial branching system. Multiple secondary branches extend from the central branch, arranged in one plane. These secondary branches give rise to tertiary shoots in the same plane, which in turn produce their new ones – all in one plane. Such a quasi-two-dimensional construction presents a convenient object for study through its two-dimensional image – a photograph. The information about the branch structure is not lost, as all elements of this structure, even the smallest ones, are clearly visible. Each shoot of the spruce branch is framed by dense rows of needles, also arranged in the plane of the branch. The optical image of a spruce branch is largely composed of the framing of branches by needles, therefore the spruce branch represents a combination of twigs and needles as a single whole.

Fig. 1 shows an image of a standard spruce branch with a small number (3–4) of branchings. We use numerical Fourier analysis technique to determine the fractal dimension of an object in two-dimensional space from its image. A photograph of a typical spruce branch is shown in Fig. 1*a*. For Fourier analysis, the image should be as contrasting as possible, ideally binary. To achieve better image contrast, branches should be photographed on a white cover on a cloudy day, or in the shade with uniform lighting, so that shadows and sunlight do not introduce additional distortions to the colors in the photograph. The shot should be taken from a distance of about 3–4 m so that the entire branch

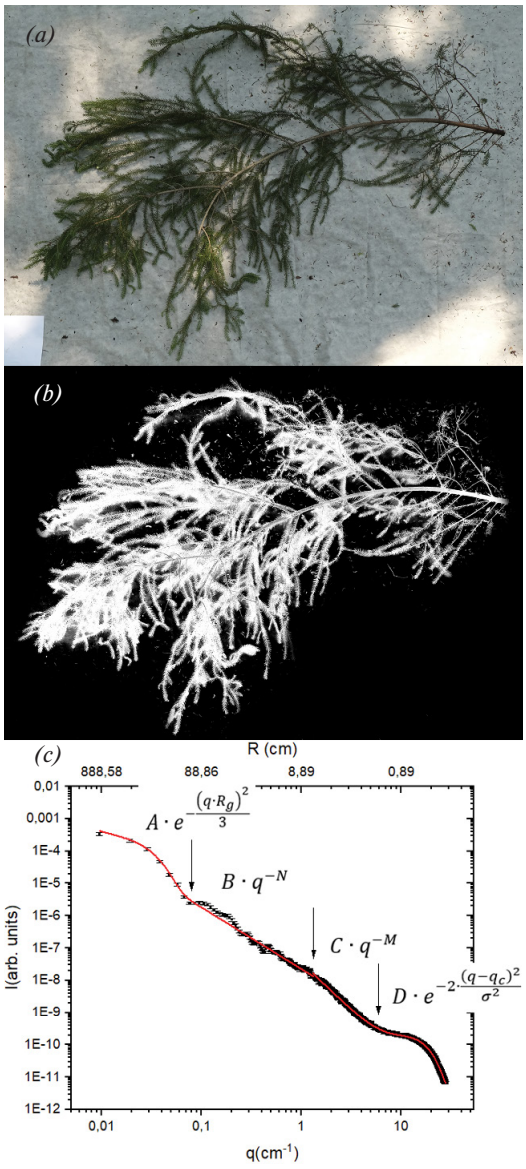

Fig. 1. Typical spruce branch (*a*), contrasting black-and-white image (*b*), dependence of spectral intensity I on transferred momentum q (Fourier dependence) (*c*)

fits in the lens. The resulting images should be processed using a graphic editor to make them as contrasting and black-and-white as possible. In addition, all extraneous objects in the photograph (stones, needles, etc.) should be painted over with a soft brush.

The contrasting black-and-white image of the same branch is shown in Fig. 1*b*. Then, numerical Fourier transform of the two-dimensional black-and-white picture is performed. The modulus of the obtained Fourier image is squared, azimuthally averaged, resulting in the dependence of spectral intensity I on momentum q (Fourier dependence) (Fig. 1*c*). To implement these steps, we used the fractal program [42]. The curve obtained from studying the image using Fourier analysis methods simulates the dependence of small-angle coherent radiation (X-ray, neutron, light) scattering intensity on the transferred momentum in reciprocal space (Fourier space), which is inversely proportional to scale. Thus, the resulting curve characterizes the amount of matter depending on scale. A more detailed description of this method and examples of its application are presented in works [34, 39, 43].

As shown in Fig. 1*c*, when studying photographs of spruce branches using numerical Fourier analysis, the scattering curve can be divided into four sections, each demonstrating its own character of intensity decrease with momentum growth. In the region of small momenta, the intensity curve is described by the Guinier function

$$I(q) \propto \exp\left(-\frac{(qR_g)^2}{3}\right)$$

with $R_g = 64 \pm 3$ cm in the range of transferred momenta from 0.01 to 0.07 cm^{-1}. In the second section, the scattering curve in double logarithmic scale is well approximated by a straight line with a slope close to 2, corresponding to the structure of a logarithmic fractal [39, 43]. This section of the curve is described by the dependence $I(q) \propto q^{-N}$ with $N = 1.90 \pm 0.03$ in the momentum range from 0.07 to 1.3 cm^{-1}, corresponding to scales in real space from 6.8 to 111 cm. The next section is characterized by accelerated intensity decrease. In double logarithmic scale, the intensity curve in this section is approximated by a straight line with a slope close to 3. In the momentum range from 1.3 to 8.5 cm^{-1} (from 1 to 6.8 cm in real space), the scattering curve is described by the law $I(q) \propto q^{-M}$ with $M = 2.95 \pm 0.01$. This section corresponds to scattering on the minimal fractal element, and the transition point from the second to the third section correlates with the size of the minimal fractal element. This dependence is essentially not fractal, both by the power index value M close to 3, and by the small range in which it is observed. This dependence characterizes the lower limit of the truly fractal range with index N in the region of small q. In the region of large transferred momenta, a characteristic feature of intensity "shoulder" with sharp cutoff at maximum q is observed. The curve

in this section is well described by the Gaussian function. In the momentum range from 8.5 cm^{-1} (less than 1 cm in real space), the scattering curve is described by the law

$$I(q) \propto \exp\left(2\frac{(q-q_c)^2}{\sigma^2}\right)$$

with $q_c = 10.3 \pm 0.1\,cm^{-1}$, corresponding to 0.86 cm in real space, and $\sigma = 13.1 \pm 1\ cm^{-1}$, corresponding to 0.68 cm in real space. This feature is associated with scattering on individual needles or their pairs, triplets – i.e., on correlations of needles framing the spruce branch. Note immediately that the spectral intensity curve of numerical Fourier transform for any spruce branches looks exactly the same and is characterized by a logarithmic fractal section and a correlation bump of spruce needles.

3. INVESTIGATION OF BRANCH IMAGES OF A 26-YEAR-OLD SPRUCE USING NUMERICAL FOURIER ANALYSIS METHODS

To demonstrate the universality of power laws characterizing spruce branch images, the numerical Fourier analysis procedure was conducted for all branches of a single spruce tree that grew in the "Orlova Roshcha" park in Gatchina, Leningrad Region. The spruce, which grew in a dense spruce forest, was blown down by wind in May 2023, after which the study was conducted. The age of the spruce was determined by counting annual rings on the trunk cross-section of the fallen tree at 40 cm from the root, which was 26 years old. The tree height was 13 meters.

Using this tree as an example, we studied the structure of branches growing at different heights of the spruce. A living branch of the fallen spruce was separated from the trunk, recording the height at which the branch grew. Then, an image (photograph) of this branch was taken, following the method and criteria described in the previous section. These photographs were processed in a graphic editor to obtain black and white images, and numerical Fourier analysis was performed using the fractal program [42].

The obtained results indicate that the spectral curves of branches taken from different heights have the same structure. Examples of branch images and their spectral curves are shown in Figs. 2–4. The first 325 cm of the trunk had no branches.

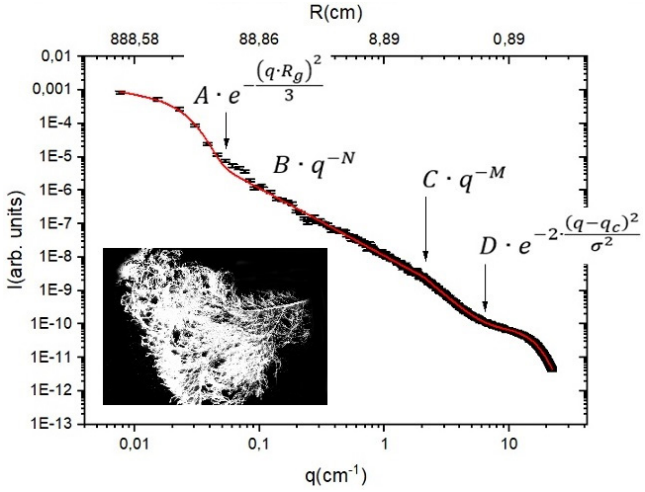

Fig. 2. Spectral curve of the spruce branch image from a height of 399 cm

Fig. 2 shows the intensity curve I from the impulse q for a spruce branch from a height of 399 cm. The dependence $I(q)$ was divided into two sections: the large-scale section at $q < 2.1\ cm^{-1}$ and the small-scale section at $q > 2.1\ cm^{-1}$. The boundary impulse $q = 2.1\ cm^{-1}$ corresponds to 4 cm in direct space. The spectral curve at large scales (small q) was described by the sum of the following two functions:

$$I(q) = A\exp\left(-\frac{(qR_g)^2}{3}\right) + Bq^{-N}. \qquad (1)$$

At $q < 0.05\ cm^{-1}$ (177 cm in direct space) the contribution from the Guinier function with radius of gyration $R_g = 86 \pm 3$ cm predominates, while at $q > 0.05\ cm^{-1}$ the contribution from the power function with power index $N = 2.02 \pm 0.02$ predominates. Such power dependence corresponds to a logarithmic fractal structure. At $q > 2.1\ cm^{-1}$ (small-scale region) the intensity curve was approximated by the sum of functions:

$$I(q) = Cq^{-M} + D\exp\left(2\frac{(q-q_c)^2}{\sigma^2}\right). \qquad (2)$$

The best approximation convergence was achieved at $M = 3.2 \pm 0.02$, $q_c = 9.1 \pm 0.1\,cm^{-1}$, $\sigma = 11.0 \pm 0.05$. At a qualitative level, it is clear that in the curve section at $q < 6.2\ cm^{-1}$ (1.4 cm in direct space) the power function dominates, while in the section at

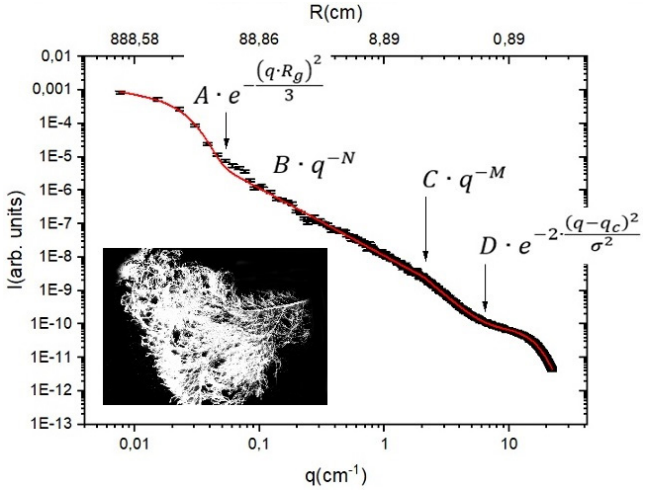

Fig. 3. Small-angle scattering curve obtained by numerical Fourier analysis of a spruce branch from a height of 663 cm

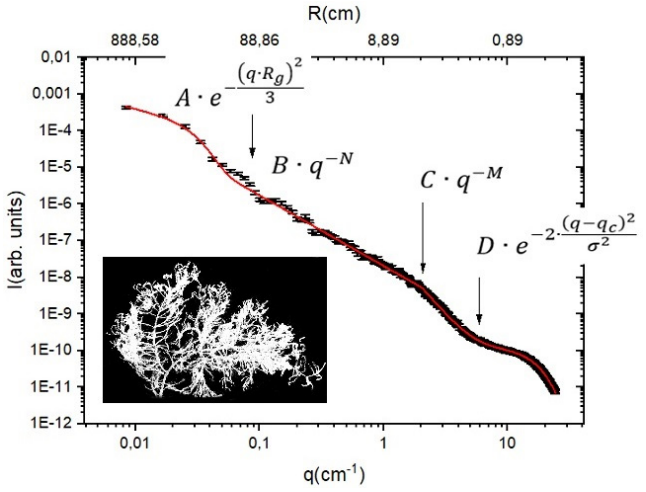

Fig. 4. Small-angle scattering curve obtained by numerical Fourier analysis of a spruce branch from a height of 830 cm

$q > 6.2$ cm^{-1} the contribution from the Gaussian function predominates. This section of the scattering curve corresponds to pair correlations of needle elements.

Fig. 3 shows the small-angle scattering curve from a spruce branch at a height of 663 cm. As in the previous case, the dependence was divided into two sections. At $q < 1.5$ cm^{-1} (6 cm in direct space) the spectral curve was described by function (1). The approximation parameters $R_g = 71 \pm 3$ cm and $N = 2.05 \pm 0.02$ are close to the values obtained in the previous case. The curve section at $q > 1.5$ cm^{-1} was described by expression (2) with characteristic parameters $M = 3.51 \pm 0.01$, $q_c = 9.0 \pm 0.1$ cm^{-1}, $\sigma = 12.4 \pm 0.2$.

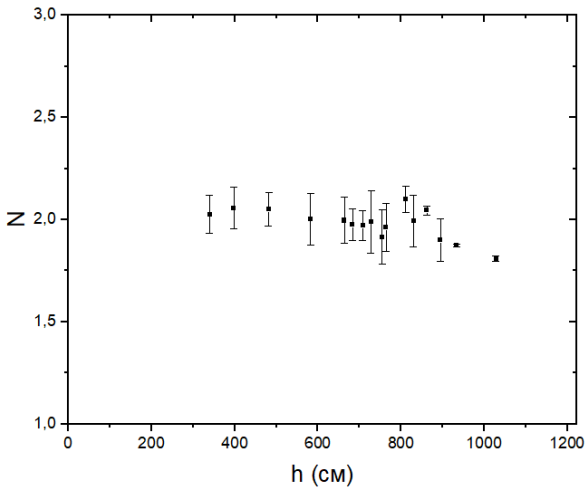

Fig. 5. Dependence of the power function exponent N on the branch growth height h

Fig. 4 shows the spectral curve for a spruce branch from a height of 830 cm. For the largescale region (small q), i.e., at $q < 1.8$ cm^{-1}, the dependence $I(q)$ was described by function (1) with parameters $R_g = 75 \pm 4$ cm and $N = 1.93 \pm 0.02$. The dependence section at $q > 1.8$ cm^{-1} was described by expression (2) with characteristic parameters $M = 3.45 \pm 0.02$, $q_c = 6.7 \pm 0.1$ cm^{-1}, $\sigma = 15.0 \pm 0.1$.

Fourier analysis of branch images growing at different heights along the tree trunk demonstrates similarity of the obtained spectral curves. All of them are characterized by a Guinier range with a gyration radius $R_g \sim 100$ cm, a wide section where the dependence q^{-N} with $N \approx 2$ is observed and maximum at $q_c \sim 9$ cm^{-1}. The value of the power exponent N depending on the branch growth height is shown in Fig. 5. According to the monopodial branching model, several branches are located at a specific trunk height. For example, at heights of 330 cm, 400 cm, and 480 cm, there were 3 branches each. The results of fractal dimension determination were averaged for each of these heights. The graph shows that along the entire length of the spruce trunk, the indicator N is close to 2. Only for branches at the top of the spruce, the indicator decreases to $\sim 1.8 - 1.9$.

There is no doubt that all branches at certain scales are characterized by the same law – a power dependence with an exponent N equal to 2, i.e., the distribution of matter in a spruce branch follows the law of logarithmic fractal. This dependence is

limited from above by the value R_g. The range in which this power dependence is observed is limited from below by the value R_{min}, separating the region of small and large scales – the transition point from dependence q^{-N} ($N \approx 2$) to dependence q^{-M} ($M \approx 3$). Fig. 6 shows the values R_g and R_{min}, characterizing the range of scales where the logarithmic fractal with $N \approx 2$ is observed. This range is approximately the same for all branches along the trunk and is limited from below by 3–4 cm, and from above by a value of about 80–100 cm. No dependence of this range on the branch growth height along the spruce trunk is observed. In fractal theory, the logarithmic fractal is characterized by a test function of the following form:

$$\rho(r) = r^2 \left(\log\frac{1}{r}\right)^{D_f}. \qquad (3)$$

The dimension of this fractal equals 2, and the value D_f is called the subdimension and equals –1. For completeness, Fig. 6 shows the dependence of parameter $R_c = 2\sqrt{2}\pi/q_c$, characterizing the distance between needles. It equals approximately 0.7 cm for all branches whose images were included in the analysis.

Thus, all spruce branches are characterized by the same dependence, described by expressions (1) and (2) with the same characteristic parameter values R_g, R_{min} and R_c.

It is interesting to compare the spectral curve for a branch with needles and for a branch without needles. Fig. 7 shows an example of a spectral curve of a spruce branch without needles. The part of the curve at $q < 2.02$ cm^{-1} is described by 1, where $R_g = 52 \pm 2$ cm, and the power exponent is $N = 1.37 \pm 0.02$. This fractal dependence, associated with the classical fractal, replaced the logarithmic fractal, thus demonstrating the qualitative difference between the structures of a branch with needles and a branch without needles. In the region of small scales, in the momentum range from 2 to 20 cm^{-1} (scale range from 0.3 to 3 cm), the spectral curve rapidly decreases, apparently characterizing the set of branch cross-sections. And the curve segment corresponding to the pair correlations of needles is completely absent.

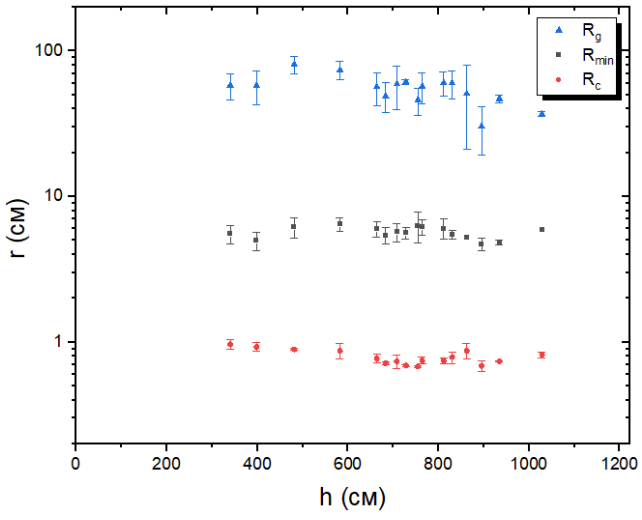

Fig. 6. Dependencies of approximation parameters R_g, R_{min}, R_s on the branch growth height h

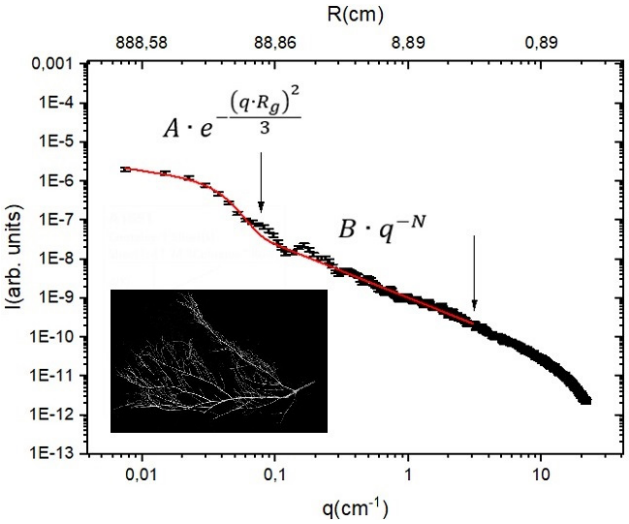

Fig. 7. Spectral curve obtained through numerical Fourier analysis of a spruce branch without needles

It is important to note that this branch lacks a structure corresponding to the logarithmic fractal, i.e., an area where there would be a dependence Q^{-2} or close to it. There is also no spectral feature characterizing needle correlations at $Q_c \approx 10$ cm^{-1}. Instead, we observe a fractal structure based on linear elements – segments of different lengths filling two-dimensional space. Overall, the object extends beyond dimension 1 and becomes an object with dimension $1 < D_f < 2$, i.e., falls under the classification of classical mass fractals in twodimensional space. Its test function in fractal theory is described by the power expression:

$$\rho(r) = r^{D_f}. \qquad (4)$$

To reliably establish the fractal dimension of a branch without needles, it is necessary to conduct a separate, statistically reliable measurement of fractality on hundreds of dry branches without needles. This research has not yet been performed. Nevertheless, we can already conclude that needles play an important role for the tree (branch) not only by themselves, but they are an important part of the structure of a living, growing branch. In other words, a branch with needles at scales ranging from 3–4 cm to 80–100 cm is a logarithmic fractal structure (according to (3)) with a flat unit element r^2. And in the same scale range, a branch without needles is described by a classical fractal with a linear unit element r (according to (4)). Looking at branch images, it is interesting to note the qualitative difference in the hierarchy of these two fractals: the hierarchy of branches by size is built from trunk to periphery, while the hierarchy of needles, conversely, is built from periphery to trunk.

4. DISCUSSION

Experimental study of the fractal properties of spruce branches using numerical Fourier analysis of their images demonstrated the presence of two fractal structures in a spruce branch at scales from 3 to 100 cm: a logarithmic fractal for the arrangement of needles on the branch and a classical mass fractal for the distribution of twigs that actually form this branch.

Without dwelling on the eternal question of which of the two fractals is primary and which is secondary, we note that for evergreen coniferous trees, the branches are framed with needles as long as they participate in the tree's vital activities. It is the needles that play the main role in forming the branch as a logarithmic fractal structure. The distribution of living matter of needles in the space of a spruce branch is not at all random. It follows the law of quasi-twodimensional fractal construction – logarithmic fractal – as if the needles are the essential, defining part of this construction. It should be reminded that in the two-dimensional case, the logarithmic fractal is interpreted as the law of equal area at different levels of spatial scaling, which in the case of a spruce branch is only fulfilled when taking into account its covering needles. This is not surprising if we consider that it is the needles, these "spruce leaves," being the carriers of photosynthesis, that serve as a source of carbon as building material for the tree's branches and trunk.

On the other hand, the distribution of needles is determined by the branching system of the limb, which is so clearly visible for a spruce branch that has no needles. A branch without needles is characterized by the structure of a classical fractal on a plane with dimension $1 < D_f < 2$. This law is random in nature and is associated with the mechanism of formation of "diffusion limited aggregation" [8].

The combination of the random nature of the classical fractal for the branch with the rigid patterns of the logarithmic fractal for needles is literally camouflaged by the high symmetry of the spruce branch structure. High symmetry is the result of genetics. The branches and top of the spruce annually repeat the same action of monopodial branching, provided by the tree's genetic code. The fact of branching for spruce has high symmetry, but the growth of new shoots is limited by the availability of resources for growth, i.e., the amount of light for photosynthesis in the needles and the amount of water and other useful components coming through the trunk and branch from the roots. That is, the fact of branching is a genetic factor, while the location of the branch, as an agglomerate of needles, in space is the result of the life process. This result is described by the law of logarithmic fractal, which implies optimal distribution of vital resources along the branch.

Let us compare our experimental results with the results of the spruce model presented in [18]. The authors (Gurtsev and Tselniker) proposed a spruce branch model based on monopodial, i.e., highly symmetrical, branching, and determined its fractal dimension based on the relationship between the total branch length and the measurement scale. In the case of an unlimited number of branchings, their obtained fractal dimension was greater than 2, not being limited by the dimensionality of space, as it should be according to fractal theory. For example, with a branch elongation factor of 0.75 and a branching coefficient of 9, they obtained a fractal dimension of 6.64. This result is explained by the fact that a branch with large branching and elongation coefficients would quickly begin to self-intersect and would fill the entire three-dimensional space several times. Such a case is impossible in the real world, but the mathematical calculations

carried out in the article did not take into account the possibility of branch self-intersections. In the case of a model with a limited branching coefficient, the fractal dimension obtained in the article was less than 2, with the fractal dimension approaching 2 as the branch grew older. Apparently, unlike the simulation model of the branch considered in article [18], a real spruce "selects" the number of branchings, elongation coefficient, and most importantly, the distribution of needles along the branch in such a way as to maintain the principle of equal matter (needles) at different branching levels. That is, the parameters of branch structure are determined by the law of logarithmic fractal distribution of needles in quasi-two-dimensional space, formed by the plane of the spruce paw.

As a result, the law of needle distribution in the branch plane is constructed to fulfill two rules of the logarithmic fractal. One of them is that the fractal has n generations, and the total areas of each generation occupied by needles in this object are equal [21]

$$d_n^2 = kd_{n+1}^2. \quad (5)$$

Here d_i is the linear size of the element of i-th generation, k is the number of branchings at each iteration. If the number of branchings at each iteration equals 4, then expression (5) can be rewritten as $d_n^2 = (2d_{n+1})^2$.

In fractal theory, the number of iterations is infinite, but in the real world it is limited. Therefore, the second condition establishes the relationship between the maximum and minimum sizes of the fractal:

$$\frac{R_{max}}{R_{min}} = \frac{nd_0}{d_n} = n2^n. \quad (6)$$

Here R_{max} is the linear size of the entire fractal, R_{min} is the linear size of the minimum element. This rule can be reformulated in a simpler form: the average density of a logarithmic fractal of the n-th generation in two-dimensional space equals $\rho_n = 1/n$. In the case of the studied spruce branches, one can estimate $n \approx 3$, i.e., the logarithmic fractal structure has 3 generations. For a model branch with a linear size of about 1 m, there are 64 spots of 3 cm size, 16 spots of 6 cm size, 4 spots of 12 cm size, and 1 spot of 24 cm size on the branch. These spots, in turn, are formed by needle agglomerates – needles.

One can roughly estimate the density of needles in black and white drawings (Figs. 2–4) by the ratio of white pixels to the total area of the drawing. This ratio equals $p = 0.33$–0.4, which also gives a value of $n = 2.5$–3.

It can be concluded that such distribution of needles in the branch space (logarithmic fractal) apparently provides maximally efficient photosynthesis within the needles and emerges as a result of tree life processes. This is particularly important given that no connection has been established between the results of metabolic scaling theory [22, 23] and experimentally obtained values of fractal dimension of trees. Our approach provides direct measurement of the fractal dimension of needle agglomerates and thereby establishes a direct link between the volumes of photosynthesis products of one branch and its fractal structure. It can be assumed that the quantitative description of spruce branch structure established in our work will allow transition to mathematically justified derivation of allometric patterns and relationships, as well as understanding of the basic processes that create these patterns.

5. CONCLUSIONS

The fractal properties of spruce branch images from a 26-year-old spruce tree approximately 13 m in length were studied at different tree heights using numerical Fourier analysis. For spruce branches photographed in different projections, a power-law dependence of spectral intensity is observed, $I(q) = Aq^{-N}$, where $N = 2$ in the range of transmitted impulses from 0.07 to 2 cm^{-1}, which corresponds to a scale in real space from 3 to 80 cm. Firstly, such a power law characterizes the scale invariance of the object's structure, i.e., the object is self-similar at different scales. Secondly, such a power law characterizes a branching structure described by a logarithmic fractal in two-dimensional space. It is shown that the logarithmic fractal structure refers to the agglomerates of needles located on the branch. Meanwhile, the branch itself – the arrangement of twigs on the branch – is described by the law of classical fractal with $1 < D_f < 2$ in the same range of transmitted impulses from 0.07 to 2 cm^{-1}. We suggested that the structure of twigs, which provides transport functions in the branch's vital activity, appears to be underlying and secondary to the distribution of needles in space, which follows the law of logarithmic fractal. The law of logarithmic

fractal in two-dimensional space is interpreted as the rule of preserving the area of needle agglomerates when changing scale: $d_i^2 = kd_{i+1}^2$, where d_i — characteristic linear size of the agglomerate i-th generation, k — number of agglomerates of the next generation.

ACKNOWLEDGMENTS

The authors are grateful to Yu. O. Chetverikov for assistance in data collection.

FUNDING

This work was supported by the Russian Science Foundation (grant No. 20-12-00188).

REFERENCES

1. B. Mandelbrot, *The Fractal Geometry of Nature, Freeman*, New York (1983).

2. Y. Kim and D. L. Jaggard, *The Fractal Random Array*, Proc. of the IEEE **74**, 1278 (1986).

3. C. Puente, *Fractal Design of Multiband Antenna Arrays*, Elec. Eng. Dept. Univ. Illinois, UrbanaChampaign, ECE 477 term project (1993).

4. C. Puente and R. Pous, *Diseco Fractal de Agrupaciones de Antenas*, IX Simposium Nacional URSI, Las Palmas **1**, 227 (1994).

5. X. Yang, J. Chiochetti, D. Papadopoulos, and L. Susman, *Fractal Antenna Elements and Arrays*, Applied Microwave and Wireless **5**, 34 (1999).

6. M. F. Barnsley, *Fractals Everywhere*, Acad. Press, Boston (1988).

7. H. O. Peitgen and P. H. Richter, *The Beauty of Fractals*, Springer, Berlin (1986).

8. E. Feder, *Fractals*, Mir, Moscow (1991).

9. V. K. Balkhanov, Yu. B. Bashkuev, *Modeling Lightning Discharges Using Fractal Geometry*, Technical Physics **82**(12), 126 (2012).

10. A. G. Bershadsky, *Fractal Structure of Turbulent Vortices*, JETP **96**, 625 (1989).

11. *Fractals in Biology and Medicine* **1**, ed. by T. F. Nonnenmacher, G. A. Losa and E. R. Weibel, Birkhäuser Verlag, Basel (1994).

12. *Fractals in Biology and Medicine* **2**, ed. by G. Losa, T. F. Nonnenmacher, D. Merlini, and E. R. Weibel, Birkhäuser Verlag, Basel (1998).

13. *Fractals in Biology and Medicine* **3**, ed. by G. Losa, D. Merlini, T. F. Nonnenmacher and E. R. Weibel, Birkhäuser Verlag, Basel (2002).

14. *Fractals in Biology and Medicine* **6**, ed. by G. Losa, D. Merlini, T. F. Nonnenmacher and E. R. Weibel, Birkhäuser Verlag, Basel (2005).

15. N. D. Lorimer, R. G. Haight, and R. A. Leary, *The Fractal Forest: Fractal Geometry and Applications in Forest Science*, General Technical Report NC-1770, Department of Agriculture, St. Paul (1994).

16. L. S. Liebovitch, *Fractals and Chaos Simplified for the Life Sciences*, Oxford Univ. Press, New York (1998).

17. I. C. Andronache, H. Ahammer, H. F. Jelineck et al., *Fractal Analysis for Studying the Evolution of Forests*, Chaos, Solitons, and Fractals **91**, 310 (2016).

18. A. I. Gurtsev, Yu. L. Tselniker, *Fractal Structure of Tree Branches*, Siberian Ecological Journal **4**, 431 (1999).

19. G. Arseniou and D. W. MacFarlane, *Fractal Dimension of Tree Crowns Explains Species Functional-Trait Responses to Urban Environments at Different Scales*, Ecological Applications **31**, 2297 (2021).

20. C. Eloy, Leonardo's Rule, *Self-Similarity and WindInduced Stresses in Trees*, Phys. Rev. Lett. **107**, 258101 (2011).

21. J. O. Indekeu and G. Fleerackers, *Logarithmic Fractals and Hierarchical Deposition of Debris*, Physica A **261**, 294 (1998).

22. G.B. West, J.H. Brown and B.J. Enquist, *A General Model for the Origin of Allometric Scaling Laws in Biology*, Science **276**, 122 (1997).

23. G. B. West, J. H. Brown, and B.J. Enquist, *A General Model for the Structure and Allometry of Plant Vascular Systems*, Nature **400**, 664 (1999).

24. D. Seidel, *A Holistic Approach to Determine Tree Structural Complexity Based on Laser Scanning Data and Fractal Analysis*, Ecology and Evolution **8**, 128 (2018).

25. Y. Malhi, T. Jackson, L. Patrick Bentley, A. Lau, A. Shenkin, M. Herold, K. Calders, H. Bartholomeus, and M.I. Disney, *New Perspectives on the Ecology of Tree Structure and Tree Communities through Terrestrial Laser Scanning*, Interface Focus **8**, 20170052 (2018).

26. S. V. Grigoriev, O. D. Shnyrkov, P. M. Pustovoit, E. G. Iashina, and K. A. Pshenichnyi, *Experimental Evidence for Logarithmic Fractal Structure of Botanical Trees*, Phys. Rev. E **105**, 044412 (2022).

27. S. V. Grigoriev, O. D. Shnyrkov, K. A. Pshenichnyi, E. G. Iashina, *Two Stages of Deciduous Tree Branching Structure Formation*, JETP **165**, 438 (2024).

28. D. D. Smith, J. S. Sperry, B. J. Enquist, V. M. Savage, K. A. McCulloh, and L. P. Bentley, *Deviation from Symmetrically Self-Similar Branching in Trees Predicts Altered Hydraulics, Mechanics, Light Interception and Metabolic Scaling*, New Phytologist **201**, 217 (2014).

29. B. Zeide, *Fractal Analysis of Foliage Distribution in Loblolly Pine Crowns,* Canad. J. Forest Res. **28**, 106 (1998).

30. B. Zeide and C. A. Gresham, *Fractal Dimensions of Tree Crowns in Three Loblolly Pine Plantations of Coastal South Carolina*, Canad. J. Forest Res. **21**, 1208 (1991).

31. B. Zeide and P. Pfeifer, *A Method for Estimation of Fractal Dimension of Tree Crowns*, Forest Sci. **37**, 1253 (1991).

32. D. Zhang, A. Samal, and J.R. Brandle, *A Method for Estimating Fractal Dimension of Tree Crowns from Digital Images*, Int. J. Pattern Recognition and Artificial Intelligence **21**, 561 (2007).

33. R. Zwiggelaar and C.R. Bull, *Optical Determination of Fractal Dimensions Using Fourier Transforms*, Opt. Eng. **34**, 1325 (1995).

34. A. A. Zinchik, Ya. B. Muzychenko, A. V. Smirnov, S. K. Stafeev, *Calculation of Fractal Dimension of Regular Fractals by Far-Field Diffraction Pattern*, Scientific and Technical Journal of ITMO University **60**, 17 (2009).

35. J. Teixeira, *Small-Angle Scattering by Fractal Systems*, J. Appl. Crystallog. **21**, 781 (1988).

36. C. Allain and M. Cloitre, *Optical Diffraction on Fractals*, Phys. Rev. B **33**, 3566 (1986).

37. J. Goodman, *Introduction to Fourier Optics*, Mir, Moscow (1970).

38. A. N. Matveev, *Optics*, Vysshaya Shkola, Moscow (1985).

39. P. M. Pustovoit, E. G. Yashina, K. A. Pshenichnyi, S. V. Grigoriev, *Classification of fractal and non-fractal objects in two-dimensional space*, Surface. X-ray, synchrotron and neutron studies **12**, 3 (2020).

40. Yu. L. Tselnikier, *Crown structure of spruce*, Forest Science **4**, 35 (1994).

41. Yu. L. Tselnikier, M. D. Korzukhin, B.B. Zeide, *Morphological and physiological studies of tree crowns*, Mir Uranii, Moscow (2000).

42. https://github.com/tre3k/fractal .

43. S. V. Grigoriev, O. D. Shnyrkov, K. A. Pshenichnyi, P. M. Pustovoit, E. G. Yashina, *Model of fractal organization of chromatin in two-dimensional space*, JETP **163**, 428 (2023).